Naval Research Laboratory

Washington, DC 20375-5320

NRL/MR/6390--13-9479

Absorption Spectra of Fe, Mn, and Mg Water Complexes Calculated Using Density Functional Theory

L. Huang
S.G. Lambrakos
N. Bernstein

Center for Computational Materials Science
Materials Science and Technology Division

A. Shabaev

George Mason University
Fairfax, Virginia

L. Massa

Hunter College, City University of New York
New York, New York

C. Yapijakis

The Cooper Union
New York, New York

August 20, 2013

REPORT DOCUMENTATION PAGE

Form Approved
OMB No. 0704-0188

1. REPORT DATE *(DD-MM-YYYY)*	2. REPORT TYPE	3. DATES COVERED *(From - To)*
20-08-2013	NRL Memorandum Report	January 4, 2013 – July 1, 2013

4. TITLE AND SUBTITLE

Absorption Spectra of Fe, Mn, and Mg Water Complexes
Calculated Using Density Functional Theory

5a. CONTRACT NUMBER

5b. GRANT NUMBER

5c. PROGRAM ELEMENT NUMBER

6. AUTHOR(S)

L. Huang, S.G. Lambrakos, N. Bernstein, A. Shabaev,[1] L. Massa,[2] and C. Yapijakis[3]

5d. PROJECT NUMBER

5e. TASK NUMBER

5f. WORK UNIT NUMBER
63-2509-S3

7. PERFORMING ORGANIZATION NAME(S) AND ADDRESS(ES)

Naval Research Laboratory, Code 6394
4555 Overlook Avenue, SW
Washington, DC 20375-5320

8. PERFORMING ORGANIZATION REPORT NUMBER

NRL/MR/6390--13-9479

9. SPONSORING / MONITORING AGENCY NAME(S) AND ADDRESS(ES)

Office of Naval Research
One Liberty Center
875 North Randolph Street, Suite 1425
Arlington, VA 22203-1995

10. SPONSOR / MONITOR'S ACRONYM(S)
ONR

11. SPONSOR / MONITOR'S REPORT NUMBER(S)

12. DISTRIBUTION / AVAILABILITY STATEMENT

Approved for public release; distribution is unlimited.

13. SUPPLEMENTARY NOTES

[1]George Mason University, Department of Computation and Data Sciences, Fairfax, VA 22030
[2]Hunter College, City University of New York, New York, NY 10065
[3]The Cooper Union, Albert Nerkin School of Engineering, New York, NY 10065

14. ABSTRACT

We present calculations of excited state resonance structure associated with Fe, Mn, and Mg water complexes using time-dependent density functional theory (TD-DFT). Calculation of excited state resonance structure using TD-DFT can provide interpretation of absorption spectra with respect to molecular structure for excitation by electromagnetic waves at frequencies within the UV range. The DFT software GAUSSIAN was used for the calculations of ground and excited state resonance structure presented here.

15. SUBJECT TERMS

Density functional theory (DFT)
Dielectric functions
Ground state resonance
Water complexes

16. SECURITY CLASSIFICATION OF:			17. LIMITATION OF ABSTRACT	18. NUMBER OF PAGES	19a. NAME OF RESPONSIBLE PERSON
a. REPORT	b. ABSTRACT	c. THIS PAGE			Samuel G. Lambrakos
Unclassified Unlimited	Unclassified Unlimited	Unclassified Unlimited	Unclassified Unlimited	24	19b. TELEPHONE NUMBER *(include area code)* (202) 767-2601

Standard Form 298 (Rev. 8-98)
Prescribed by ANSI Std. Z39.18

Contents

1. Introduction……...……..…….…....1

2. Calculation of Absorption Spectra using DFT……..……..…….…….2

3. Physical Significance of Quantum Mechanical Transition State for Molecular Transformation…....4

4. Excited State Resonance Structure of Fe, Mn and Mg Water Complexes…….…..4

5. Conclusion…….…….……..5

6. References……...…….…..…..……....5

7. Appendix. Stable geometries of Fe++ ·6(H2O) showing no UV excitations according to TD-DFT..8

Introduction

The present study is based on significant progress in density functional theory (DFT), and associated software technology, which is sufficiently mature for the determination of dielectric response structure, and should actually provide complementary information to that obtained from experiment. Calculations are presented of excited state resonance structure associated with Fe, Mn and Mg water complexes using time-dependent density functional theory (TD-DFT), which is an extension of DFT. Calculation of excited state resonance structure using TD-DFT can provide interpretation of absorption spectra with respect to molecular structure for excitation by electromagnetic waves at frequencies within the UV range. In principle, these absorption spectra should provide quantitative initial estimates of spectral response features that can be subsequently adjusted with respect to additional information such as laboratory measurements and other types of theory based calculations, or conversely, adapted as constraints for the inverse analysis of experimentally measured absorption spectra. A significant aspect of using DFT and TD-DFT for the calculation of absorption spectra is that it adopts the perspective of computational physics, according to which a numerical simulation represents another source of "experimental" data.

Density functional theory has been successfully used to investigate the vibrational spectra of energetic materials in the form of single molecules and molecular crystals [1-9]. These calculations provide interpretation of absorption spectra with respect to molecular structure for various forms of materials, which can be encountered in various detection scenarios. In particular, the calculated absorption spectra of isolated molecules can help to identify intramolecular vibrational modes of various materials. A series of studies have focused on the general concept of constructing dielectric response functions using DFT for the purpose of quantitative simulation of explosives detection scenarios [9,10,11]. For these studies the DFT software GAUSSIAN09 (G09) was adopted [12]. As emphasized in these studies, the calculation of absorption spectra using DFT and TD-DFTdefines a general approach where dielectric response is estimated within the bounds of relatively well-defined adjustable parameters. Following this approach, permittivity functions are constructed using DFT and TD-DFT calculated absorption spectra under the condition that the calculated resonance locations are fixed, while resonance widths and number densities are assumed adjustable with respect to additional information such as experimentally observed spectra or more advanced theory.

Previous studies have examined various properties of water molecules and their clusters [13-21]. The absorption spectrum of molecular clusters consisting of water molecules should be of significance for interpretation of absorption spectra associated with detection in practice. This follows in that most environments associated with detection in practice include the presence of water in one form or another. These forms can range from isolated molecules in gas phase, molecular clusters, adsorbed surface layers, droplets and interface regions in liquid phase, and ice. Absorption spectra of metal-water complexes represent an important case for dielectric response with respect to electromagnetic wave excitation. This regime should be better quantified for improved interpretation of absorption spectra associated with systems that include metal-water complexes as components.

The organization of the subject areas presented are as follows. First, a general review of the elements of vibrational analysis using DFT for determination the stability of molecular geometies is presented. Second, a brief discussion presedented concerning the significance of imaginary frequencies for vibrational analysis using DFT. Third, the excited state resonance structure of Fe, Mn and Mg water complexes is investigated using TD-DFT calculations. Finally, a conclusion is given.

Manuscript approved July 11, 2013.

Calculation of Absorption Spectra using DFT

As in previous studies [9, 10, 11] the formal mathematical structure underlying DFT calculations, as well as the procedure for calculation of absorption spectra corresponding to vibrational states, is included here for purposes of completeness. The extension of DFT for the calculation of absorption spectra corresponding to electronic excitation states, which is the formalism of time-dependent density functional theory (TD-DFT), is described in reference [22]. In this study, we consider the calculation of absorption spectra for electronic excitation states. The calculation of absorption spectra for vibrational states is considered, however, for the purpose of investigating the stability of molecular geometries. With respect to the relative stability of molecular geometries, the significance of imaginary frequencies is discussed below.

The DFT software GAUSSIAN09 (G09) can be used to compute an approximation of the IR absorption spectrum of a molecule or molecules [23]. This program calculates vibrational frequencies by determining second derivatives of the energy with respect to the Cartesian nuclear coordinates, and then transforming to mass-weighted coordinates at a stationary point of the geometry. The IR absorption spectrum is obtained using density functional theory to compute the ground state electronic structure in the Born-Oppenheimer approximation using Kohn-Sham density functional theory [24-29]. GAUSSIAN uses specified orbital basis functions to describe the electronic wavefunctions and density. For a given set of nuclear positions, the calculation directly gives the electronic charge density of the molecule, the potential energy *V*, and the displacements in Cartesian coordinates of each atom. The procedure for vibrational analysis followed in GAUSSIAN is that described in Ref [23]. Reference [29] presents a fairly detailed review of this procedure. A brief description of this procedure is as follows.

The procedure followed by GAUSSIAN is based on the fact the vibrational spectrum depends on the Hessian matrix $\mathbf{f}_{\mathrm{CART}}$, which is constructed using the second partial derivatives of the potential energy *V* with respect to displacements of the atoms in Cartesian coordinates. Accordingly, the elements of the *3N* x *3N* matrix $\mathbf{f}_{\mathrm{CART}}$ are given by

$$f_{\mathrm{CART}\,ij} = \left(\frac{\partial^2 V}{\partial \xi_i \partial \xi_j} \right)_0 \qquad \text{(Eq 1)}$$

where $\{\xi_1, \xi_2, \xi_3, \xi_4, \xi_5, \xi_6, ..., \xi_{3N}\} = \{\Delta x_1, \Delta y_1, \Delta z_1, \Delta x_2, \Delta y_2, \Delta z_2, ..., \Delta z_N\}$, which are displacements in Cartesian coordinates, and *N* is the number of atoms. As discussed above, the zero subscript in Eq.(1) indicates that the derivatives are taken at the equilibrium positions of the atoms, and that the first derivatives are zero. Given the Hessian matrix defined by Eq.(1) the operations for calculation of the vibrational spectrum require that the Hessian matrix Eq.(1) be transformed to mass-weighted Cartesian coordinates according to the relation

$$f_{\mathrm{MWC}\,ij} = \frac{f_{\mathrm{CART}\,ij}}{\sqrt{m_i m_j}} = \left(\frac{\partial^2 V}{\partial q_i \partial q_j} \right)_0 \qquad \text{(Eq 2)}$$

where $\{q_1, q_2, q_3, q_4, q_5, q_6, ..., q_{3N}\} = \left\{\sqrt{m_1}\Delta x_1, \sqrt{m_1}\Delta y_1, \sqrt{m_1}\Delta z_1, \sqrt{m_2}\Delta x_2, \sqrt{m_2}\Delta y_2, \sqrt{m_2}\Delta z_2, ..., \sqrt{m_N}\Delta z_N\right\}$ are the mass-weighted Cartesian coordianates. GAUSSIAN computes the energy second derivatives Eq.(2), thus computing the forces for displacement perturbations of each atom along each Cartesian direction. The first derivatives of the dipole moment with respect to atomic positions $\partial \vec{\mu} / \partial \xi_i$ are also computed. Each vibrational eigenmode leads to one peak in the absorption spectrum, at a frequency equal to the mode's eigenfrequency ν_{n0}. The absorption intensity corresponding to a particular eigenmode *n* whose eigenfrequency is ν_{n0} is given by

$$I_n = \frac{\pi}{3c} \left| \sum_{i=1}^{3N} \frac{\partial \vec{\mu}}{\partial \xi_i} l_{\mathrm{CART}\,in} \right|^2, \qquad \text{(Eq 3)}$$

where $\mathbf{l}_{CART}$ is the matrix whose elements are the displacements of the atoms in Cartesian coordinates. The matrix $\mathbf{l}_{CART}$ is determined by the following procedure. First,

$$\mathbf{l}_{CART} = \mathbf{M}\mathbf{l}_{MWC} , \quad \text{(Eq 4)}$$

where $\mathbf{l}_{MWC}$ is the matrix whose elements are the displacements of the atoms in mass-weighted Cartesian coordinates and **M** is a diagonal matrix defined by the elements

$$M_{ii} = \frac{1}{\sqrt{m_i}} . \quad \text{(Eq 5)}$$

Proceeding, $\mathbf{l}_{MWC}$ is the matrix needed to diagonalize $\mathbf{f}_{MWC}$ defined by Eq.(2) such that

$$(\mathbf{l}_{MWC})^T \mathbf{f}_{MWC}(\mathbf{l}_{MWC}) = \Lambda , \quad \text{(Eq 6)}$$

where Λ is the diagonal matrix with eigenvalues λ_i. The procedure for diagonalizing Eq.(6) consists of the operations

$$\mathbf{f}_{INT} = (\mathbf{D})^T \mathbf{f}_{MWC}(\mathbf{D}) \quad \text{(Eq 7)}$$

and

$$(\mathbf{L})^T \mathbf{f}_{MWC}(\mathbf{L}) = \Lambda , \quad \text{(Eq 8)}$$

where **D** is a matrix transformation to coordinates where rotation and translation have been separated out and **L** is the transformation matrix composed of eigenvectors calculated according to Eq.(8). The eigenfrequencies in units of (cm^{-1}) are calculated using the eigenvalues λ_n by the expression

$$\nu_{n0} = \frac{\sqrt{\lambda_n}}{2\pi c} , \quad \text{(Eq 9)}$$

where *c* is the speed of light. The elements of $\mathbf{l}_{CART}$ are given by

$$l_{CARTki} = \sum_{j=1}^{3N} \frac{D_{kj} L_{ji}}{\sqrt{m_j}}, \quad \text{(Eq 10)}$$

where *k, i=1,..., 3N,* and the column vectors of these elements are the normal modes in Cartesian coordinates.

The intensity Eq.(3) must then be multiplied by the number density of molecules to give an absorption-line intensity in the non-interacting molecule approximation. It follows that the absorption spectrum calculated by GAUSSIAN is a sum of delta functions, whose line positions and coefficients correspond to the vibrational-transition frequencies and the absorption-line intensities, respectively. In principle, however, these spectral components must be broadened and shifted to account for anharmonic effects such as finite mode lifetimes and inter-mode couplings.

The DFT software GAUSSIAN09 (G09) can be used to compute an approximation of the UV absorption spectrum of a molecule or molecules by application of the formalism of time-dependent density functional theory (TD-DFT), which is described in reference [22].

Physical Significance of Quantum Mechanical Transition State for Molecular Transformation

A molecule in 3-dimensions has a total of 3N-6 normal mode vibrations. The Schrodinger equation for the harmonic oscillations of these normal modes has known solutions. The quantum mechanical spectrum of each of these vibrations is given in the harmonic approximation by the energies $E_n = (n+1/2)h\nu$, where n is a quantum number, h is Planck's constant, and ν is a vibration frequency given by $\nu=\sqrt{(k/m)}$, where k is the spring constant of the normal vibration and m is the effective mass contributed by those atoms vibrating in the normal mode. A molecule in stable equilibrium is characterized by all positive normal mode frequencies ν. But the definitive mathematical characteristic of a transition state is that it has all positive frequencies but one, which is imaginary. That is to say, (k/m) is a negative number. The vibration corresponding to an imaginary frequency is one in which the atoms are breaking away from bonds characteristic of chemical reactants and are moving towards those bonds characteristic of chemical products. Chemical reactions break bonds in the reactants, rearrange them and form new bonds in the products. The transition state is a particular geometric arrangement of the atoms in a chemical system, at the maximal peak of the energy surface separating reactants from products. In the transition state every normal vibration distortion but one, occurs within a stable energy minimum. But the one normal mode distortion of imaginary frequency occurs at an unstable energy maximum sending reactants toward products. The height of energy peak, the activation energy E_a, associated with the occurrence of a transition state determines the minimal energy accumulated by reactants to surmount the barrier separating reactants from products. In the Arrhenius formulation, the rate constant for the reaction is given by $\Gamma = A\, e^{-Ea/RT}$, where A is a constant, R is the ideal gas constant, and T is the absolute temperature. The common occurrence is that a particular transition state mechanism for chemical reaction is associated with one imaginary frequency, and therefore a single mechanism of reaction. Much less commonly, an energy surface of multiple channels of reaction mechanism may give rise to correspondingly multiple imaginary frequencies. But in any event, the transition state contains the energetic and geometric information that defines the transformation inherent within chemical reactions.

Excited State Resonance Structure of Fe, Mn and Mg Water Complexes

In this section are presented the results of computational investigations using DFT and TD-DFT concerning Fe, Mn and Mg water complexes of various size. These results include the relaxed or equilibrium configurations of metal-water complexes, denumeration of imaginary frequencies for stability analysis of molecular geometries, which are calculated by DFT, and oscillator strength as a function of excitation energy (within the UV range) for different geometries of the interacting systems associated with stable structures, which are calculated by TD-DFT. For these calculations geometry optimization and vibrational analysis was effected using the DFT model B3LYP [30, 31] and basis function 6-31G(d,p) [32, 33]. According to the specification of this basis function, (d,p) designates polarization functions having one set of d and p functions for heavy atoms and hydrogen atoms, respectively [34].

A graphical representation of Fe, Mn, Mg water complexes having different molecular geometries and sizes are shown in Figs. (1) through (25). Given in Tables 1 through 5 are excitation energies and oscillator strenghts for various molecular geometries, sizes, and electronic structures of Fe, Mn, Mg water complexes with and without water background after geometry optimization calculated using TD-DFT. Given in Table 6 are total energies for optimized geometries and denumeration of imaginary frequencies for calculation of vibrational (IR) spectra using DFT (B3LYP/6-31G(d,p)) for Mn water complexes. Shown in the appendix are the geometrie of $Fe^{++}\cdot 6H_2O$ (D_{3d}) and (D_{4h}) corresponding to stable structures (see Figs. (A1) and (A2)). For these geometries TD-DFT calculations predict that there are no UV excitations.

Conclusion

The TD-DFT calculated absorption spectra given here provide two types of information for general analysis of dielectric response. These are the denumeration of excited state resonance modes and estimates of molecular level dielectric response structure. The calculations of excited state resonance structure associated with Fe, Mn and Mg water complexes using TD-DFT are meant to serve as reasonable estimates of molecular level response characteristics, providing interpretation of dielectric response features, for subsequent adjustment relative to experimental measurements and additional constraints based on molecular structure theory. With respect to spectroscopic methods for detection or monitoring of target molecules within various types of water environments, i.e., different types of detection strategies and their associated algorithms for post-processing of measurements, the calculated resonance spectra presented here serve the purpose of isolating spectral features for correlating with the presence of metal water complexes.

Acknowledgement

Funding for this project was provided by the Office of Naval Research (ONR) through the Naval Research Laboratory's Basic Research Program.

References

[1] B. M. Rice and C. F. Chabalowski, "Ab Initio and Nonlocal Density Functional Study of 1,3,5-Trinitro-s-triazine (RDX) Conformers,``J. Phys. Chem., **101**, 8720 (1997).

[2] Y. Chen, H. Liu, Y. Deng, D. Schauki, M. J. Fitch, R. Osiander, C. Dodson, J. B. Spicer, M. Shur, and X.-C. Zhang, "THz spectroscopic investigation of 2,4-dinitrotoluene," Chemical Physics Letters, **400**, 357-361 (2004).

[3] D. G. Allis, D. A. Prokhorova, and T. M. Korter, "Solid-State Modeling of the Terahertz Spectrum of the High Explosive HMX," J. Phys. Chem. A., **110**, 1951-1959 (2006).

[4] D.G. Allis and T. M. Korter, "Theoretical Analysis of the Terahertz Spectrum of the High Explosive PETN," Chem. Phys. Chem., **7**, 2398 (2006).

[5] J. Chen, Y. Chen, H. Zhao, G. J. Bastiaans, and X.-C. Zhang, Opt. Exp., **15**, 11763 (2007).

[6] M.R. Leahy-Hoppa, M.J. Fitch, X. Zheng, L.M. Hayden, and R. Osiander, "Wideband terahertz spectroscopy of explosives," Chemical Physics Letters **434**, 227-230 (2007).

[7] J. Hooper, E. Mitchell, C. Konek, and J. Wilkinson, "Terahertz spectroscopy techniques for explosives detection," Chem. Phys. Lett., **467**, 309 (2009).

[8] M.R. Leahy-Hoppa, M.J. Fitch, and R. Osiander,"Terahertz spectroscopy techniques for explosives detection," Anal. Bioanal. Chem., **395**, 247 (2009).

[9] A. Shabaev, S. G. Lambrakos, N. Bernstein, V. L. Jacobs and D. Finkenstadt, "A General Framework for Numerical Simulation of Improvised Explosive Device (IED)-Detection Scenarios Using Density Functional Theory (DFT) and Terahertz (THz) Spectra," Appl. Spectroscopy, **65**, 409 (2011).

[10] A. Shabaev, S.G., Lambrakos, N. Bernstein, V. Jacobs, D. Finkenstadt, "THz Dielectric Properties of High Explosives Calculated by Density Functional Theory for the Design Of Detectors," Journal of Materials Engineering and Performance, DOI: 10.1007/s11665 011-9857-8, 20 (9), 2011, p.1536.

[11] L. Huang, A. Shabaev, S.G. Lambrakos, N. Bernstein, V. Jacobs, D. Finkenstadt, L. Massa, "Dielectric Response of High Explosives at THz Frequencies Calculated Using Density Functional Theory," Journal of Materials Engineering and Performance, 2011, DOI: 10.1007/s11665-011-0020-3.

[12] M. J. Frisch, G. W. Trucks, H. B. Schlegel, G. E. Scuseria, M. A. Robb, J. R. Cheeseman, G. Scalmani, V. Barone, B. Mennucci, G. A. Petersson, H. Nakatsuji, M. Caricato, X. Li, H. P. Hratchian, A. F. Izmaylov, J. Bloino, G. Zheng, J. L. Sonnenberg, M. Hada, M. Ehara, K. Toyota, R. Fukuda, J. Hasegawa, M. Ishida, T. Nakajima, Y. Honda, O. Kitao, H. Nakai, T. Vreven, J. A. Montgomery, Jr., J. E. Peralta, F. Ogliaro, M. Bearpark, J. J. Heyd, E. Brothers, K. N. Kudin, V. N. Staroverov, R. Kobayashi, J. Normand, K. Raghavachari, A. Rendell, J. C. Burant, S. S. Iyengar, J. Tomasi, M. Cossi, N. Rega, J. M. Millam, M. Klene, J. E. Knox, J. B. Cross, V. Bakken, C. Adamo, J. Jaramillo, R. Gomperts, R. E. Stratmann, O. Yazyev, A. J. Austin, R. Cammi, C. Pomelli, J. W. Ochterski, R. L. Martin, K. Morokuma, V. G. Zakrzewski, G. A. Voth, P. Salvador, J. J. Dannenberg, S. Dapprich, A. D. Daniels, Ö. Farkas, J. B. Foresman, J. V. Ortiz, J. Cioslowski, and D. J. Fox, Gaussian 09, Revision A.1, Gaussian, Inc., Wallingford CT, 2009.

[13] M. W. Mahoney and W. L. Jorgensen, "A five-site model for liquid water and the reproduction of the density anomaly by rigid, nonpolarizable potential functions, *J. Chem. Phys.*, Vol. 112, No. 20 (2000), pp 8910-22.

[14] W. L. Jorgensen, J. Chandrasekhar, J. D. Madura, R.W. Impey and M. L. Klein, "Comparison of simple potential functions for simulating liquid water," *J. Chem. Phys.,* Vol. 79, No. 2, 1983, pp. 926-935.

[15] T. James, D. J. Wales, J. Hernandez-Rojas, "Global minima for water clusters $(H_2O)_n$, $n \leq 21$, described by a five-site empirical potential," Chemical Physics Letters 415 (2005), pp 302–307.

[16] D. J. Wales and M. P. Hodges, "Global minima of water clusters ($H_2O)_n$, $n \leq 21$, described by an empirical potential," Chemical Physics Lett., 286 (1998), pp 65-72.

[17] Jer-Lai Kuo and W. F. Kuhs, "A First Principles Study on the Structure of Ice-VI: Static Distortion, Molecular Geometry, and Proton Ordering," J. Phys. Chem., B 2006, 110, pp. 3697-3703.

[18] M. W. Mahoney and W. L. Jorgensen, "Quantum, intramolecular flexibility, and polarizability effects on the reproduction of the density anomaly of liquid water by simple potential functions," J. Chem. Phys., Vol. 115, No. 23, 2001, pp. 10758-10768.

[19] S. Maheshwary, N. Patel, and N. Sathyamurthy, A. D. Kulkarni and S. R. Gadre, "Structure and Stability of Water Clusters $(H2O)_n$, n=8-20: An Ab Initio Investigation," J. Phys. Chem. A, 2001, 105, pp. 10525-10537.

[20] H. M. Lee, S. B. Suh, and K. S. Kima, "Structures, energies, and vibrational spectra of water undecamer and dodecamer: An ab initio study," J. Chem. Phys., Vol. 114, No. 24, 2001,

pp.10749-10756.

[21] X. Li, X. Xu, D. Yuang and X. Weng, "Hexagonal prismatic dodecameric water cluster: a building unit of the five-fold interpenetrating six-connected supramolecular network," Chem. Commun., 2012, 48, pp. 9014-9016.

[22] E. Runge and E.K.U. Gross, "Density Functional Theory for Time-Dependent Systems," Phys. Rev. Lett., 52 (12), 1984, pp.997-1000.

[23] A. Frisch, M. J. Frisch, F. R. Clemente and G. W. Trucks, *Gaussian 09 User's Reference,* Gaussian Inc., 2009, p, 105-106, online: www.gaussian.com/g_tech/g_ur/g09help.htm

[24] P. Hohenberg and W. Kohn, "Inhomogeneous Electron Gas" Phys. Rev. **136**, B864, (1964).

[25] W. Kohn and L. J. Sham, "Self-Consistent Equations Including Exchange and Correlation Effects" Phys. Rev. **140**, A1133 (1965).

[26] R.O. Jones and O. Gunnarson, "The density functional formalism, its applications and prospects" Rev. Mod. Phys. **61**, 689 (1989).

[27] R. M. Martin, *Electronic Structures Basic Theory and Practical Methods*, Cambridge University Press, Cambridge 2004, p. 25.

[28] E. B. Wilson, J. C. Decius and P. C. Cross, *Molecular Vibrations* (McGraw-Hill, New York, 1955).

[29] J.W. Ochterski, "Vibrational Analysis in Gaussian," help@gaussian.com, 1999.

[30] A. D. Becke, "Density-functional Thermochemistry. III. The Role of Exact Exchange"*, J. Chem. Phys.* **98**, 5648-5652 (1993).

[31] B. Miehlich, A. Savin, H. Stoll and H. Preuss, "Results Obtained with the Correlation Energy Density Functionals of Becke and Lee, Yang and Parr", Chem. *Phys. Lett.* **157**, 200-206 (1989).

[32] A. D. McLean and G. S. Chandler, "Contracted Gaussian-basis sets for molecular calculations. 1. 2nd row atoms, Z=11-18," *J. Chem. Phys.*, **72** 5639-48 (1980).

[33] T. Clark, J. Chandrasekhar, G. W. Spitznagel and P. V. R. Schleyer, "Efficient diffuse function-augmented basis-sets for anion calculations. 3. The 3-21+G basis set for 1st-row elements, Li-F," *J. Comp. Chem.*, **4** 294-301, (1983).

[34] M. J. Frisch, J. A. Pople and J. S. Binkley, "Self-Consistent Molecular Orbital Methods. 25. Supplementary Functions for Gaussian Basis Sets," *J. Chem. Phys.*, **80** (1984) 3265-69.

Appendix. Stable geometries of $Fe^{++}\cdot 6(H_2O)$ showing no UV excitations according to TD-DFT

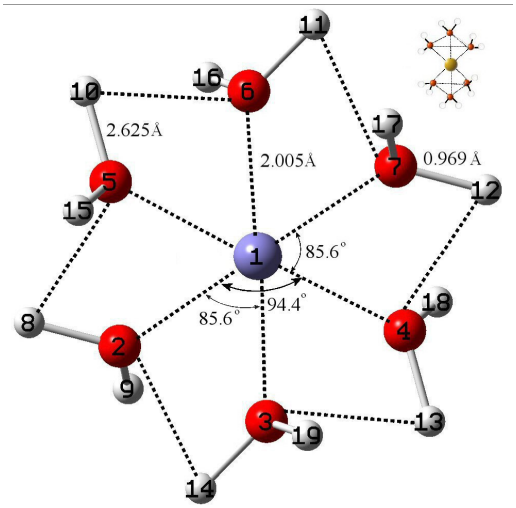

Figure A1. Molecular geometry of $Fe^{++}\cdot 6H_2O$ (D_{3d}) corresponding to stable structure. For this geometry there is no UV excitation.

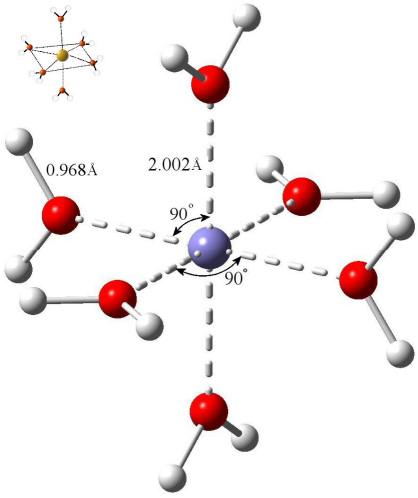

Figure A2. Molecular geometry of $Fe^{++}\cdot 6H_2O$ (D_{4h}) corresponding to stable structure. For this geometry there is no UV excitation.

Table 1. Excitation energies and oscillator strenghts for $\mathbf{Fe^{++} \cdot 3(H_2O)}$ and $\mathbf{Fe \cdot 3(H_2O)}$ after geometry optimization calculated using TD-DFT.

Complex	Excitation Energy	Oscillator Strength	Complex	Excitation Energy	Oscillator Strength
$\mathbf{Fe^{++} \cdot 3(H_2O)}$	847.83 nm 831.67 nm 667.04 nm	0.0003 0.0004 0.0005	$\mathbf{Fe^{++} \cdot 3(H_2O)}$ **in water**	1958.26 nm 1560.28 nm 762.19 nm 707.94 nm 641.34 nm	0.0001 0.0001 0.0002 0.0002 0.0003
$\mathbf{Fe \cdot 3(H_2O)}$	609.82 nm	0.0326	$\mathbf{Fe \cdot 3(H_2O)}$ **in water**	637.73 nm	0.0356

Table 2. Excitation energies and oscillator strenghts for $\mathbf{Fe^{++} \cdot 5(H_2O)}$ after geometry optimization calculated using TD-DFT (B3LYP/6-31G(d,p)).

Complex	Excitation Energy	Oscillator Strength	Complex	Excitation Energy	Oscillator Strength
$\mathbf{Fe^{++} \cdot 5(H_2O)}$ $\mathbf{(D_{3d})}$	2007.74 nm 514.92 nm 484.82 nm	0.0001 0.0004 0.0004	$\mathbf{Fe^{+2} \cdot 5(H_2O)}$ $\mathbf{(D_{3d})}$ **In water**	1473.84 nm 1322.75 nm 489.22 nm 467.55 nm	0.0002 0.0001 0.0002 0.0003

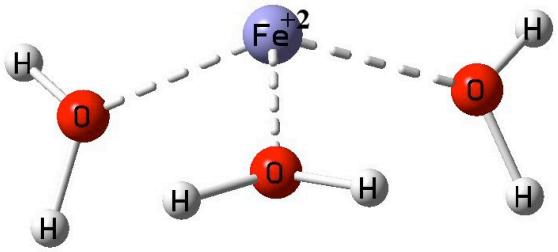

Figure 1. Molecular geometry of $Fe^{++} \cdot 3H_2O$ corresponding to stable structure.

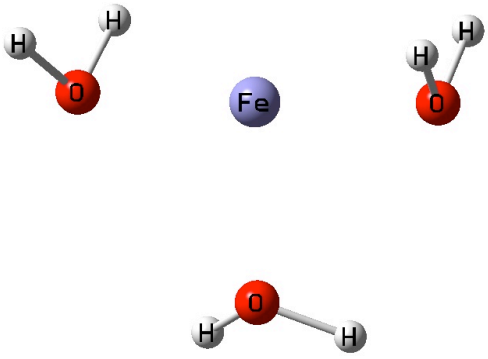

Figure 2. Molecular geometry of $Fe \cdot 3H_2O$ corresponding to stable structure.

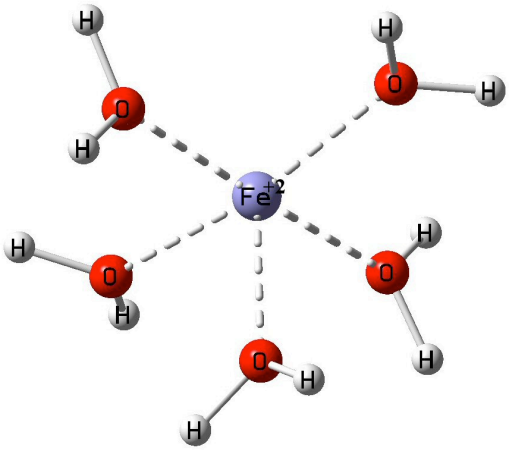

Figure 3. Molecular geometry of $Fe^{++} \cdot 5(H_2O)$ (D_{3d}) corresponding to stable structure.

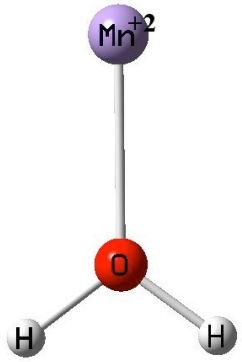

Figure 4. Molecular geometry of $Mn^{+2} \cdot H_2O$ corresponding to stable structure. For both doublet and singlet multiplicity there is no UV excitation.

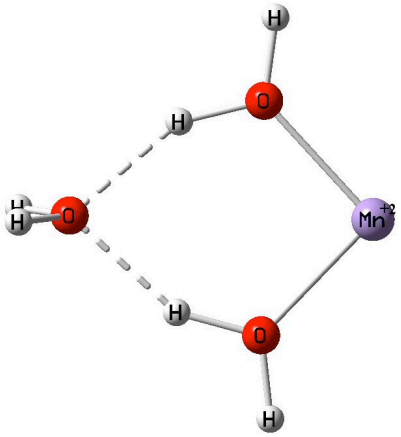

Figure 5. Molecular geometry of $Mn^{+2} \cdot 3H_2O$ corresponding to stable structure. For the case of doublet multiplicity there is no UV excitation.

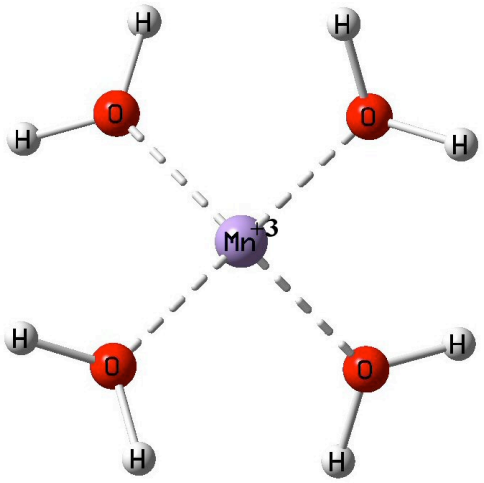

Figure 6. Molecular geometry of $Mn^{+3} \cdot 4H_2O$ corresponding to stable structure. For the case of singlet multiplicity there is UV excitation.

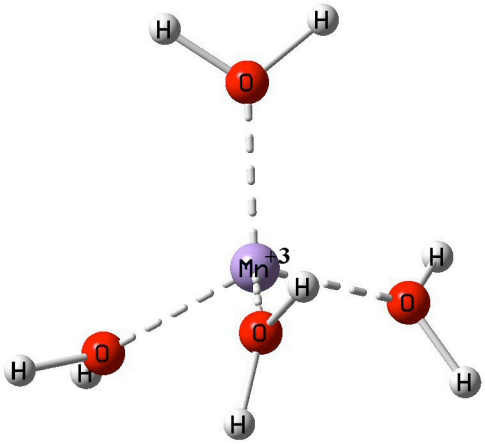

Figure 7. Molecular geometry of $Mn^{+3} \cdot 4H_2O$ corresponding to stable structure. For the case of singlet multiplicity there is UV excitation.

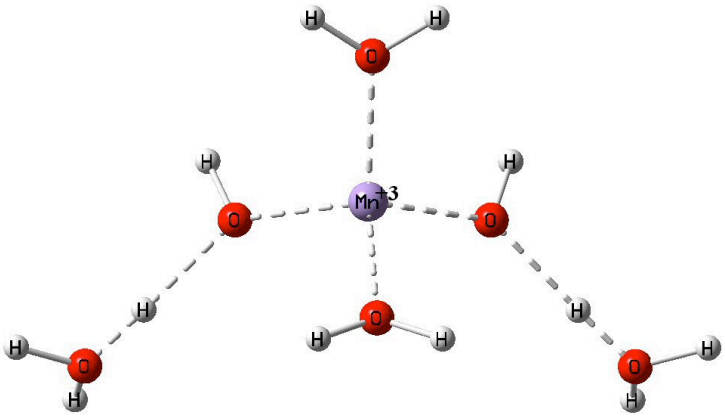

Figure 8. Molecular geometry of $Mn^{+3} \cdot 6H_2O$ corresponding to stable structure. For the case of singlet multiplicity there is UV excitation.

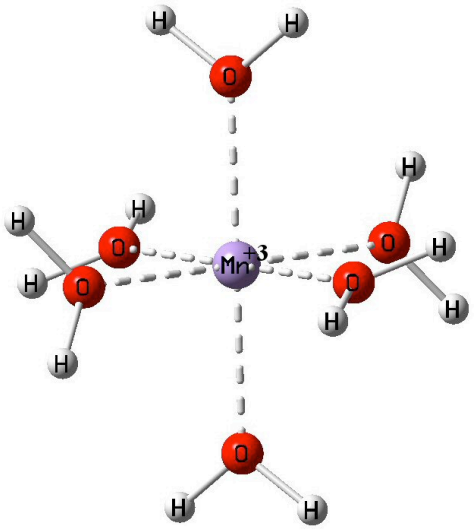

Figure 9. Molecular geometry of $Mn^{+3} \cdot 6H_2O$ corresponding to stable structure. For the case of singlet multiplicity there is UV excitation.

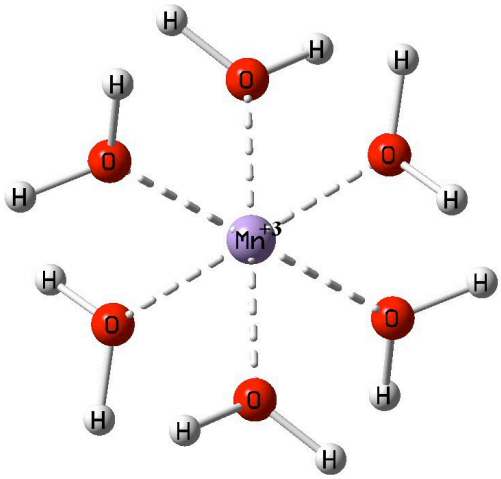

Figure 10. Molecular geometry of $Mn^{+3} \cdot 6H_2O$ corresponding to stable structure. For the case of singlet multiplicity there is no UV excitation.

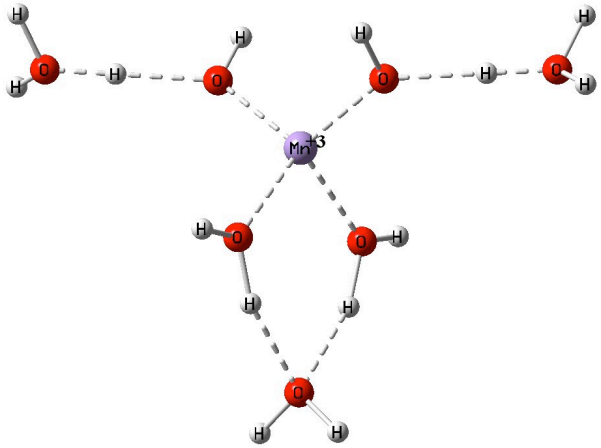

Figure 11. Molecular geometry of $Mn^{+3} \cdot 7H_2O$ corresponding to stable structure. For the case of singlet multiplicity there is UV excitation.

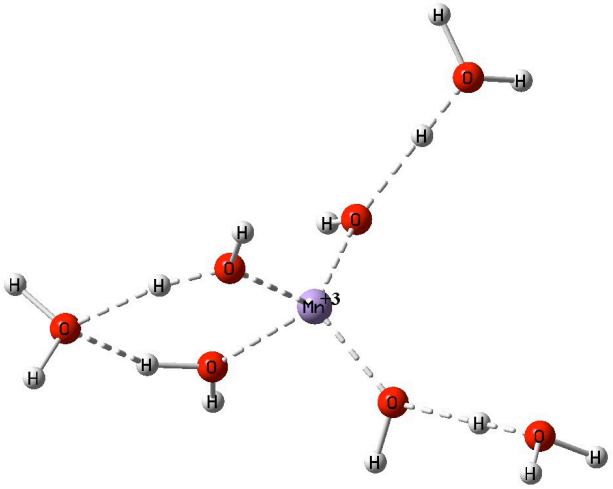

Figure 12. Molecular geometry of $Mn^{+3} \cdot 7H_2O$ corresponding to stable structure. For the case of singlet multiplicity there is UV excitation.

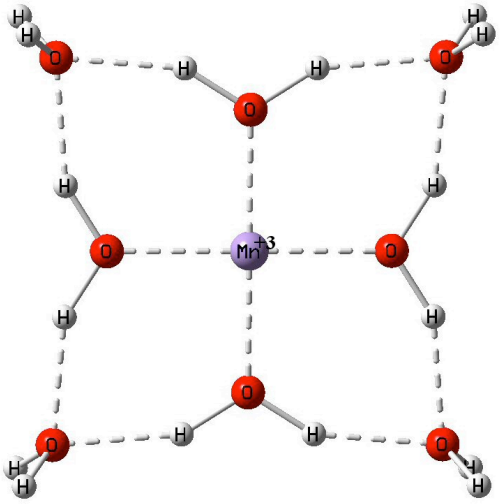

Figure 13. Molecular geometry of $Mn^{+3} \cdot 8H_2O$ corresponding to stable structure. For the case of singlet multiplicity there is UV excitation.

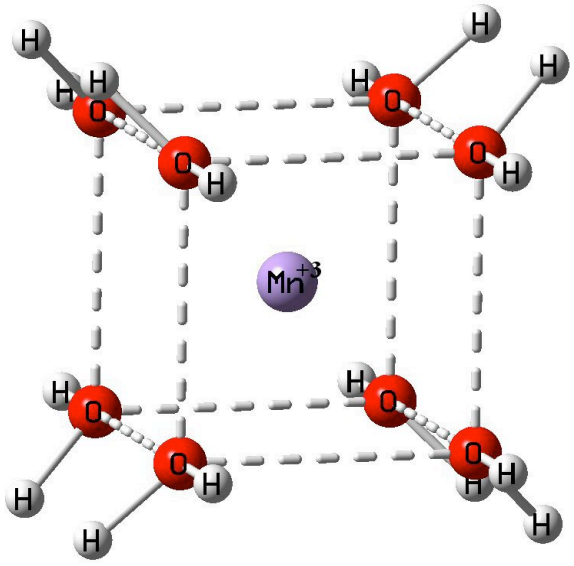

Figure 14. Molecular geometry of $Mn^{+3} \cdot 8H_2O$ corresponding to stable structure. For the case of singlet multiplicity there is no UV excitation.

Table 3. Excitation energies and oscillator strenghts for $Mn^{+2} \cdot n(H_2O)$ (doublet) and $Mn^{+3} \cdot n(H_2O)$ (singlet) after geometry optimization calculated using TD-DFT (B3LYP/6-31G(d,p)).

$Mn^{+2} \cdot n(H_2O)$ (doublet)			**$Mn^{+3} \cdot n(H_2O)$ (singlet)**		
$n(H_2O)$	Excitation E	Oscillator strength	**$n(H_2O)$**	Excitation E	Oscillator strength
n =1	no peak	Oscillator strength = 0	**n = 1**	no peak	Oscillator strength = 0
n = 2	Unstable geometry		**n = 2**	Unstable geometry	
	Unstable geometry				
n = 3	no peak	Oscillator strength = 0	**n = 3**	Unstable geometry	
n = 4	None (Convergence criterion not met)		**n = 4**	348.11 nm	0.0137
				1112.09 nm 1111.13 nm 773.28 nm 625.73 nm 625.08 nm	0.0002 0.0002 0.0016 0.0024 0.0024
n = 5	None (Convergence criterion not met)			Unstable geometry	
				Unstable geometry	
n = 6	Unstable geometry		**n = 6**	Unstable geometry	
				Unstable geometry	
				762.69 nm 759.70 nm 717.17 nm 514.02 nm	0.0007 0.0012 0.0022 0.0029
				no peak	Oscillator strength = 0
				no peak	Oscillator strength = 0
n = 7	None (Convergence criterion not met)		**n = 7**	904.18 nm 751.21 nm 671.68 nm 542.40 nm	0.0001 0.0023 0.0014 0.0036
				1177.44 nm 982.24 nm 614.12 nm 561.69 nm	0.0002 0.0017 0.0013 0.0013
n = 8	None (Convergence criterion not met)		**n = 8**	no peak	Oscillator strength = 0
				Unstable geometry	
n = 12	None (Convergence criterion not met)		**n = 12**	Unstable geometry	

Table 4. Excitation energies and oscillator strenghts for $Mg^{+2} \cdot n(H_2O)$ with and without water background after geometry optimization calculated using TD-DFT (B3LYP/6-31G(d,p)).

Componds	Excitation E	Oscillator strength	Componds	Excitation E	Oscillator strength
$Mg^{+2} \cdot 1(H_2O)$	233.27 nm 136.24 nm 124.18 nm 120.26 nm 114.83 nm	0.0080 0.0590 0.1341 0.0409 0.0110	**$Mg^{+2} \cdot 1(H_2O)$ in water**	157.32 nm 124.55 nm 112.92 nm 109.63 nm	0.0288 0.0156 0.0020 0.1892
$Mg^{+2} \cdot 2(H_2O)$	175.98 nm 175.98 nm 124.41 nm	0.0201 0.0201 0.0079	**$Mg^{+2} \cdot 2(H_2O)$ in water**	152.17 nm 152.17 nm 127.18 nm 127.18 nm	0.0341 0.0341 0.0117 0.0117
$Mg^{+2} \cdot 3(H_2O)$	152.88 nm 152.14 nm 121.01 nm	0.0303 0.0588 0.0432	**$Mg^{+2} \cdot 3(H_2O)$ in water**	147.99 nm 147.35 nm 127.31 nm 126.89 nm	0.0443 0.0732 0.0189 0.0083
$Mg^{+2} \cdot 4(H_2O)$	-	-	**$Mg^{+2} \cdot 4(H_2O)$ in water**	-	-
$Mg^{+2} \cdot 5(H_2O)$	146.59 nm 144.31 nm 143.31 nm 142.12 nm	0.0236 0.0782 0.0609 0.0501	**$Mg^{+2} \cdot 5(H_2O)$ in water**	148.60 nm 146.13 nm 144.94 nm 144.94 nm	0.0553 0.0605 0.0560 0.0705
$Mg^{+2} \cdot 6(H_2O)$	725.79 nm 144.97 nm 144.97 nm 144.97 nm	0.3477 0.0940 0.0940 0.0940	**$Mg^{+2} \cdot 6(H_2O)$ in water**	146.83 nm 146.83 nm 146.83 nm	0.1048 0.1048 0.1048

Table 5. Excitation energies and oscillator strenghts for Mg· n(H_2O) with and without water background after geometry optimization calculated using TD-DFT (B3LYP/6-31G(d,p)).

Componds	Excitation E	Oscillator strength	Componds	Excitation E	Oscillator strength
Mg ·1(H_2O)	341.28 nm 333.85 nm 320.04 nm 207.67 nm 198.23 nm 166.73 nm	0.5217 0.5312 0.5599 0.1132 0.0029 0.0299	**Mg ·1(H_2O) in water**	373.21 nm 371.06 nm 362.03 nm 208.95 nm 192.17 nm 172.23 nm	0.5508 0.0029 0.5677 0.0870 0.0031 0.0318
Mg ·2(H_2O)	378.26 nm 372.02 nm 372.02 nm 201.22 nm 201.22 nm	0.6040 0.4846 0.4846 0.0079 0.0079	**Mg ·2(H_2O) in water**	423.86 nm 422.77 nm 422.77 nm 198.18 nm 198.18 nm	0.6413 0.5068 0.5068 0.0116 0.0116
Mg ·3(H_2O)	-	-	**Mg ·3(H_2O) in water**	-	-
Mg ·4(H_2O)	354.06 nm 335.15 nm 313.65 nm 226.00 nm 209.57 nm 198.68 nm	0.5032 0.4924 0.4655 0.0377 0.0015 0.0283	**Mg ·4(H_2O) in water**	390.51 nm 371.33 nm 346.89 nm 234.66 nm 216.34 nm 203.49 nm	0.5549 0.4807 0.4895 0.0343 0.0089 0.0302
Mg ·5(H_2O)	593.22 nm 541.31 nm 535.79 nm 327.91 nm 281.44 nm 264.19 nm	0.2000 0.4545 0.3704 0.0631 0.0693 0.0084	**Mg ·5(H_2O) in water**	517.52 nm 506.00 nm 475.78 nm 292.27 nm 259.25 nm 234.97 nm	0.4093 0.5147 0.1890 0.0279 0.0984 0.0005
Mg ·6(H_2O)	725.79 nm 725.79 nm 725.79 nm 307.15 nm	0.3477 0.3477 0.3477 0.0045	**Mg ·6(H_2O) in water**	820.34 nm 820.34 nm 820.34 nm 303.45 nm	0.3865 0.3865 0.3865 0.0037

Table 6. Total energy for optimized geometry and denumeration of imaginary frequencies for calculation of vibrational (IR) spectra using DFT (B3LYP/6-31G(d,p)).

Mn^{+2} · n(H2O) (doublet)			Mn^{+3} · n(H2O) (singlet)		
	Energy_opt (a.u.)	**Imag. Freq.**		**Energy_opt (a.u.)**	**Imag. Freq.**
n =1	-1226.400	0	**n = 1**	-1225.472	0
n = 2	-1302.970	1	**n = 2**	-1302.139	1
	-1302.957	1			
n = 3	-1379.465	0	**n = 3**	-1378.696	1
n = 4	None (Convergence criterion not met)		**n = 4**	-1455.351	0
				-1455.353	0
n = 5	None (Convergence criterion not met)		**n = 5**	-1531.868	1
				-1531.850	3
n = 6	-1608.982	1	**n = 6**	-1608.374	2
				-1608.373	4
				-1608.401	0
				-1608.392	0
				-1608.392	0
n = 7	None (Convergence criterion not met)		**n = 7**	-1684.898	0
				-1684.896	0
n = 8	None (Convergence criterion not met)		**n = 8**	-1761.365	0
				-1761.213	17
n = 12	None (Convergence criterion not met)		**n = 12**	-2067.146	6

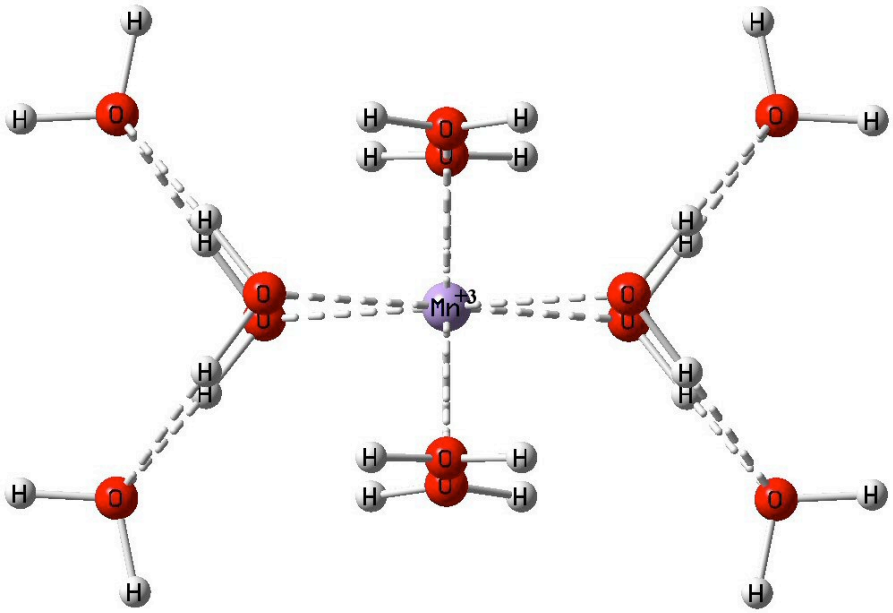

Figure 15. Molecular geometry of $Mn^{+3} \cdot 12H_2O$ corresponding to stable structure. For the case of singlet multiplicity there is no UV excitation.

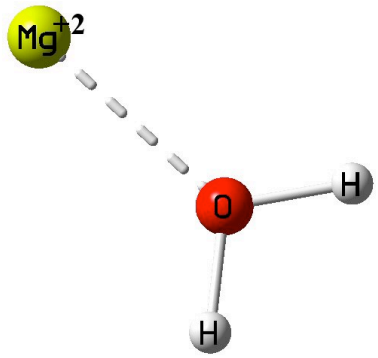

Figure 16. Molecular geometry of $Mg^{+2} \cdot 1(H_2O)$ corresponding to stable structure. For this structure there is UV excitation.

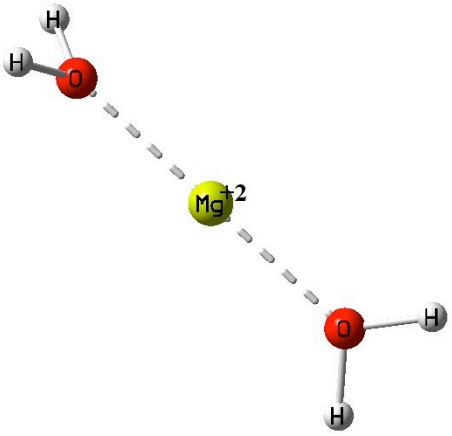

Figure 17. Molecular geometry of $Mg^{+2} \cdot 2(H_2O)$ corresponding to stable structure. For this structure there is UV excitation.

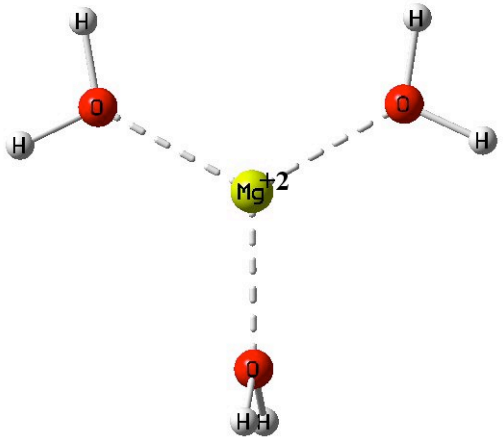

Figure 18. Molecular geometry of $Mg^{+2} \cdot 3(H_2O)$ corresponding to stable structure. For this structure there is UV excitation.

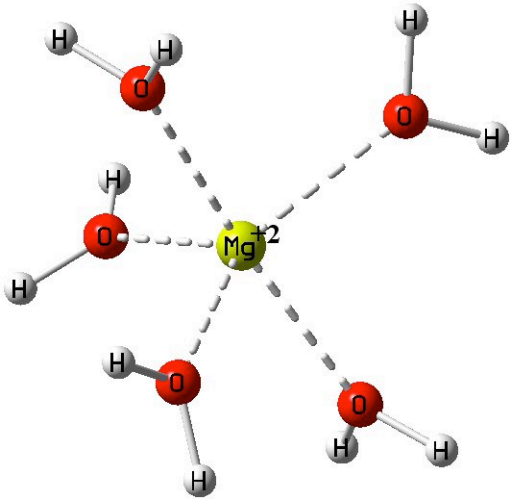

Figure 19. Molecular geometry of $Mg^{+2} \cdot 5(H_2O)$ corresponding to stable structure. For this structure there is UV excitation.

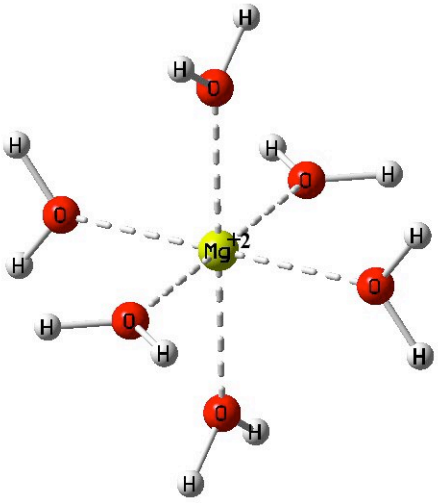

Figure 20. Molecular geometry of $Mg^{+2} \cdot 6(H_2O)$ corresponding to stable structure. For this structure there is UV excitation.

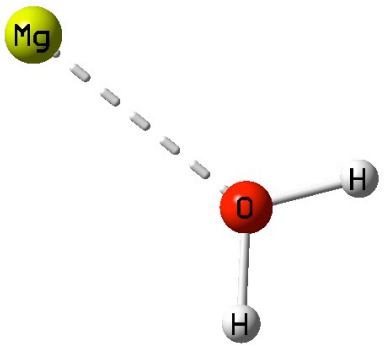

Figure 21. Molecular geometry of Mg·1(H_2O) corresponding to stable structure. For this structure there is UV excitation.

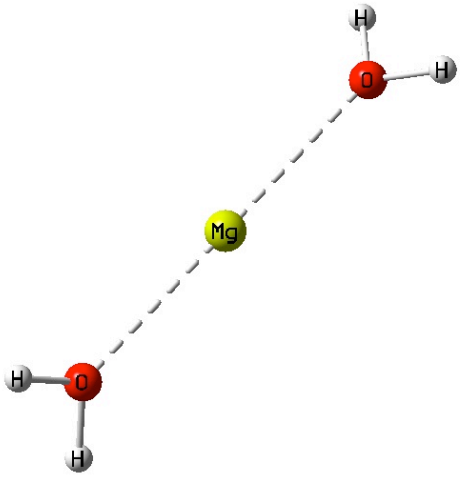

Figure 22. Molecular geometry of Mg·2(H_2O) corresponding to stable structure. For this structure there is UV excitation.

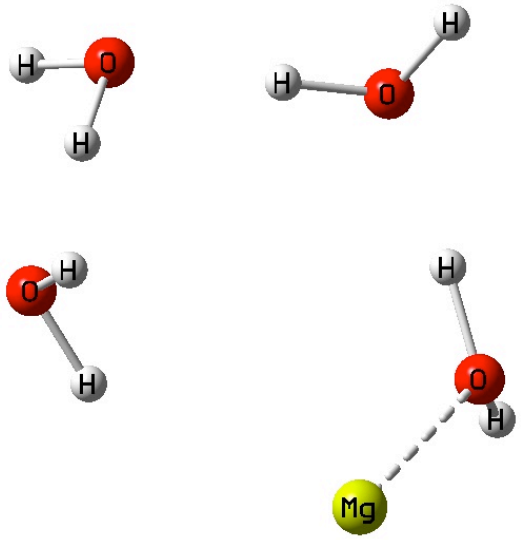

Figure 23. Molecular geometry of Mg·4(H_2O) corresponding to stable structure. For this structure there is UV excitation.

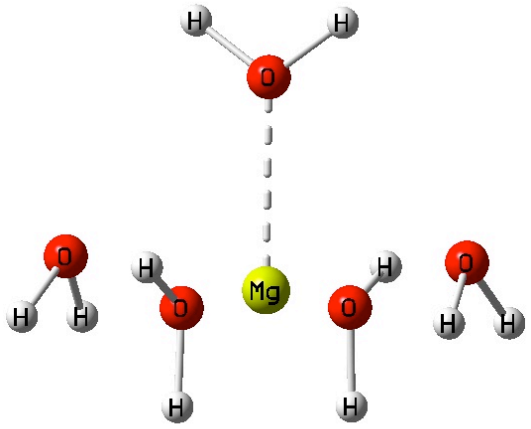

Figure 24. Molecular geometry of $Mg \cdot 5(H_2O)$ corresponding to stable structure. For this structure there is UV excitation.

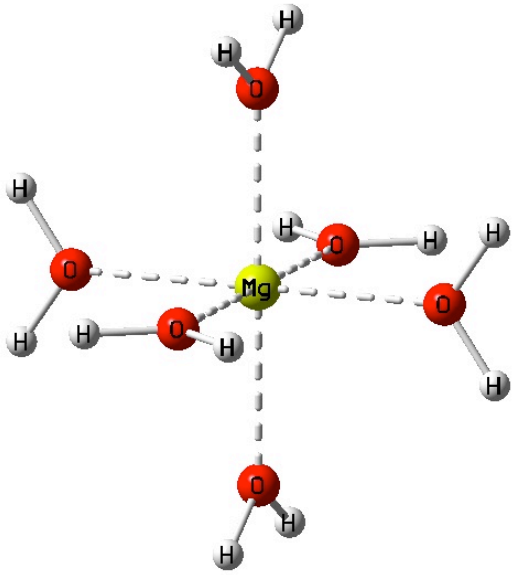

Figure 25. Molecular geometry of $Mg \cdot 6(H_2O)$ corresponding to stable structure. For this structure there is UV excitation.